Journal of Rehabilitation in Civil Engineering 8-4 (2020) 01-14

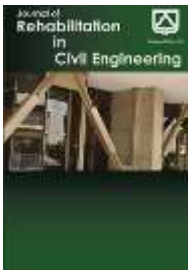

journal homepage: http://civiljournal.semnan.ac.ir/

Prediction of Service Life in Concrete Structures based on Diffusion Model in a Marine Environment Using Mesh Free, FEM and FDM Approaches

A. Farahani[1*] and H. Taghaddos[2]
1. Assistant Professor, Department of Civil Engineering, Tafresh University, Tafresh, Iran
2. Assistant Professor, School of Civil Engineering, University of Tehran, Tehran, Iran

Corresponding author: *afarahani@tafreshu.ac.ir*

ARTICLE INFO

Article history:
Received: 07 February 2020
Accepted: 24 May 2020

Keywords:
Concrete,
Diffusion,
Element-Free Galerkin (EFG),
Finite Element Method (FEM),
Finite Difference Method (FDM).

ABSTRACT

Chloride-induced corrosion is a key factor in the premature corrosion of concrete structures exposed to a marine environment. Fick's second law of diffusion is the dominant equation to model diffusion of chloride ions. This equation is traditionally solved by Finite Element Method (FEM) and Finite Difference Method (FDM). Although these methods are robust and efficient, they may face some numerical issues due to discretization process. This study solves the Fick's equation using the Element-Free Galerkin (EFG) method as well as traditional FEM and FDM. The results of these numerical methods are compared together, and validated with the analytical solution in special cases. The results show that the EFG method predicts the service life of the concrete structures, more accurately than the other methods, and exhibits the lowest displacement error and energy error for a constant diffusion coefficient problem. FDM can be performed very efficiently for simple models, and the displacement errors produced by this method do not differ considerably from the EFG results. Therefore, FDM could compete with the EFG method in simple geometries. FEM can be used with a sufficient number of elements while the convergence of the results should be controlled. However, in complicated models, FEM and especially the EFG method are much more flexible than FDM.

1. Introduction

Contamination of concrete with chloride ions is one of the main causes of the premature corrosion of reinforced concrete structures in a marine environment [1, 2]. The service life of these structures can be determined based on the initiation time of the corrosion of steel bars due to chloride penetration [2-5]. If the amount of chloride at the level of the steel

DOI: 10.22075/JRCE.2020.19189.1380

bars reaches a particular threshold value of chloride, the passive layer on the steel bar is destroyed and the corrosion process begins. In the other words, the initiation time is the time takes to penetrate sufficient chloride into the concrete cover thickness and initiate corrosion process [6]. Thus, reliable methods for predicting chloride ingress into concrete are required to prevent the deterioration of new structures and determine the condition of existing ones. Traditionally, numeric mesh-based methods such as Finite Element Method (FEM) [7] and Finite Difference Method (FDM) [8] are employed to model diffusion process. However, generating a mesh is not only computationally expensive, but it is also subject to a number of error sources, such as discontinuity of the field variable and locking derivation [9]. Thus, numerous mesh-free methods have been developed in the recent years for solving Partial Differential Equations (PDEs) [9]. Global domain discretization in MeshLess Methods (MLM) is performed based on a set of geometrically unconnected nodes instead of a mesh of discrete elements. Various types of meshless methods based on different formulations have been developed for different applications. Some of these methods are based on the global weak form. These weak form methods include Diffuse Element Method (DEM) [10], the Element-Free Galerkin method (EFG) [11], Reproducing Kernel Particle Method (RKPM) [12], Partition of Unity Finite Element Method (PUFEM) [13] and the Meshless Galerkin method based on Radial Basis Functions (MGRBF) [14-16]. Some other meshless methods e.g. the General Finite Difference Method (GFDM) with arbitrary mesh [17] and Finite Point Method (FPM) [18] have been developed based on the global strong form. In this paper, the EFG method is employed to solve the diffusion equation, and the results are compared to FEM, FDM and analytical method in special cases.

2. Chloride Diffusion Model

The diffusion of chloride ions is generally assumed to follow Fick's Second Law of diffusion [3] is presented in Eq. (1).

$$\frac{\partial C}{\partial t} = D.\nabla^2 C \tag{1}$$

where, C (in percentage) is the chloride content in concrete, D (in m^2/s) is the chloride diffusion coefficient and t (in days) is the current exposure time.

Farahani et al. [19] have presented an empirical model for the chloride diffusion coefficient of silica fume concrete in the tidal zone of a marine site located in Bandar Abbas, a port city in the southern region of Iran. This model, presented in Eq. (2) and Eq. (3), predicts the chloride diffusion coefficient based on time, temperature, silica fume content and water-to-binder ratio for the marine environments located in tidal zone of south side of Iran.

$$D(t,Temp) = D_{ref}\left(\frac{t_{ref}}{t}\right)^m \exp\left[\frac{U}{R}\left(\frac{1}{Temp_{ref}} - \frac{1}{Temp}\right)\right] \tag{2}$$

$$D_{ref} = (-4.0 + 18.1(w/b) + 1.81(w/b)^2 - 0.1SF + 0.02SF^2 - 0.86(w/b \times SF)) \times 10^{-12} \tag{3}$$

where, D (in m^2/s) is the chloride diffusion coefficient, D_{ref} (in m^2/s), presented in Eq. (3), is the reference diffusion coefficient at the reference time (90 days), t (in days) is the current exposure time, t_{ref} is the reference time (90 days), $Temp$ (in Kelvin) is the current temperature, $Temp_{ref}$ is the reference temperature (307.3 K), m is the age factor (m = 0.24) representing the time dependence of

the chloride diffusion coefficient [20], U (in $J.mol^{-1}$) is the activation energy of the diffusion process, R is the gas constant ($8.314\ J.mol^{-1}.K^{-1}$), w/b is the water-to-binder ratio ($0.35 \leq w/b \leq 0.50$) and SF (in percent) is the silica fume content as a replacement of Portland cement content in the concrete mixtures. The value of U/R ratio for the south of Iran is estimated 2948 K [21-23].

In this study, various proportions of the mixtures were produced by changing the water-to-binder ratios: w/b (0.35, 0.40, 0.45 and 0.50) and the silica fume contents: SF (5%, 7.5%, 10% and 12.5%). The mixture proportions of these concrete mix designs are summarized in Table 1.

Table 1. Concrete mixture composition [18].

w/b	Ratio	*SF*	Content (%)	Water (kg/m^3)	Cement (kg/m^3)	*SF* (kg/m^3)	Fine aggregates (kg/m^3)	Coarse aggregates (kg/m^3)	Superplasticizer (kg/m^3)
W1	0.35	SF1	5.0	140	380	20	931	968	-
	0.35	SF2	7.5	140	370	30	931	968	6.0
	0.35	SF3	10.0	140	360	40	906	968	6.4
	0.35	SF4	12.5	140	350	50	929	964	4.8
W2	0.40	SF1	5.0	160	380	20	833	1018	3.6
	0.40	SF2	7.5	160	370	30	832	1017	3.2
	0.40	SF3	10.0	160	360	40	830	1014	3.6
	0.40	SF4	12.5	160	350	50	829	1012	3.8
W3	0.45	SF1	5.0	180	380	20	810	990	1.2
	0.45	SF2	7.5	180	370	30	808	998	2.0
	0.45	SF3	10.0	180	360	40	807	985	1.8
	0.45	SF4	12.5	180	350	50	806	983	2.0
W4	0.50	SF1	5.0	200	380	20	793	991	0.8
	0.50	SF2	7.5	200	370	30	784	959	1.2
	0.50	SF3	10.0	200	360	40	820	1020	1.8
	0.50	SF4	12.5	200	350	50	782	955	2.0

3. Solving Diffusion Equation

This section investigates the diffusion equation solution by FDM, FEM and EFG methods. The theory of each method is explained and formulated below:

3.1. FDM

FDM solves the diffusion equation by providing a grid of nodes. A comprehensive discussion of the FDM method can be found in reference [24].

Eq. (4) provides a solution of diffusion equation for one-dimensional (1D) problems, such as a plane sheet with thickness L. To ensure the stability of the procedure, the grid size should be small enough to satisfy Eq. (5).

$$C_{i,n+1} = C_{i,n} + D\frac{\delta t}{(\delta x)^2}(C_{i-1,n} - 2C_{i,n} + C_{i+1,n}) \quad (4)$$

$$D\frac{\delta t}{(\delta x)^2} \le \frac{1}{2} \quad (5)$$

where, the region space-time (x-t) is covered by a grid of rectangles of side δx, δt, and the value of the chloride concentration (C) at the grid point (x, t), with coordinate of ($i\delta x$, $n\delta t$), is denoted by $C_{i,n}$.

This method can be easily extended for two-dimensional (2D) cases by covering a rectangular space grid of side δx, δy at each time step, δt. Eq. (6) provides a solution of the diffusion equation for a 2D problem. Similar to the previous case, the grid size in Eq. (6) should satisfy the constraint defined in Eq. (7) to ensure stability.

$$C_{i,j,n+1} = C_{i,j,n} + D\delta t\left(\frac{C_{i-1,j,n} - 2C_{i,j,n} + C_{i+1,j,n}}{(\delta x)^2} + \frac{C_{i,j-1,n} - 2C_{i,j,n} + C_{i,j+1,n}}{(\delta y)^2}\right) \quad (6)$$

$$D\delta t\left(\frac{1}{(\delta x)^2} + \frac{1}{(\delta y)^2}\right) \le \frac{1}{2} \quad (7)$$

where, the coordinate of a representative grid point (x, y) at time ($t = n\delta t$) is denoted by ($i\delta x$, $j\delta y$), and the value of C at such grid point is denoted by $C_{i,j,n}$.

3.2. FEM

A number of previous studies have proposed FEM algorithms to solve an advection (convection) diffusion equation [3, 24, 25]. In the present study, the diffusion equation, without the additional term of advection, is solved by using FEM. Because, FEM is a base method of element-free methods, the effective stiffness matrix and the effective force vector are derived using a Galerkin weak form approach.

The diffusion equation for a 1D problem can be represented in the Cartesian coordinate system by discretizing the domain into 1D smaller elements (1D mesh) and dividing the time interval [0, t] into a finite number of equal subintervals Δt. Therefore, the chloride content at the end of the nth time interval, denoted by C^{n+1}, is derived according to Eq. (8).

$$\mathbf{K_{eff}}\,\Delta\vec{C}^{\,n+1} = \vec{P}_{eff} \quad (8)$$

where, the terms $\mathbf{K_{eff}}$, $\Delta\vec{C}^{\,n+1}$ and $\vec{P}_{eff}$ are the effective stiffness matrix, the difference between chloride content at the end of the n+1th and nth time intervals and the effective force vector, respectively.

Similarly for 2D problems, the FEM discretizes a domain into small 2D mesh elements (e.g. triangle) and divides the time interval [0, t] into a finite number of equal subintervals Δt.

3.3. EFG

Similar to FEM, the EFG method also employs the Galerkin weak form formulation. However, the main difference is the formulation of the shape function. In contrary to the FEM that employ mesh to

discretize a domain, meshless methods such as EFG do not discretize the domain with elements. EFG employs Moving Least Square (MLS) technique, to generate the shape functions. The central idea of MLS is that a global approximation can be achieved by going through a "moving" process. Therefore, for each integration point, a list of nodes, including the integration points, is required. Then, all the non-zero contributions in the Galerkin equations are evaluated. The vectors are evaluated over a specified domain of influence and then assembled. The result is a local matrix for the integration points, which should be assembled into the global matrix. The solution of the problem is obtained by solving the global system of equations [26].

3.3.1. Galerkin Weak Form

To summarize, applying the Galerkin method to the diffusion equation results in:

$$\begin{bmatrix} \mathbf{K_{eff}} & \mathbf{G} \\ \mathbf{G}^{\mathrm{T}} & 0 \end{bmatrix} \begin{bmatrix} \Delta \vec{C}^{\,n+1} \\ \vec{\lambda} \end{bmatrix} = \begin{bmatrix} \vec{P}_{eff} \\ \vec{q} \end{bmatrix} \quad (9)$$

where, the terms $\mathbf{K_{eff}}$, $\Delta \vec{C}^{\,n+1}$, $\vec{P}_{eff}$, $\mathbf{G}$, $\vec{q}$ and $\vec{\lambda}$ can be calculated.

Eq. (9) indicates the general format of Eq. (8); these are used for the EFG shape functions. For the integration over the entire domain Ω, a background mesh must be used. To simplify the procedure and for the sake of comparison with FEM, the same FEM mesh is used as the background mesh.

3.4. Analytical Solution (Constant Diffusion Coefficient)

The analytical solution, in a 1D domain, can be obtained by using the variables separation method. To set the parameters, a constant diffusion coefficient, a domain with thickness of L and the following initial conditions (IC) and boundary conditions (BC) are assumed:

IC: $C = 0,\ 0 < x < L,\ t = 0$,

BC: $C = C_0, x = 0,\ x = L,\ t > 0$ (10)

where, C_0 is the chloride concentration on the concrete surface (assumed to be constant). The closed form solution results in [2]:

$$C = C_0 - \frac{4C_0}{\pi} \sum_{n=0}^{\infty} \frac{1}{2n+1} \exp\left\{ -D\left(\frac{(2n+1)\pi}{L} \right)^2 t \right\} \sin \frac{(2n+1)\pi x}{L} \quad (11)$$

Similarly, in a rectangular domain with side lengths of L and H, the following initial and boundary conditions are assumed:

IC: $C = 0$, $0 < x < L$, $0 < y < H$, $t = 0$,

BC: $C = C_0,\ x = 0,\ x = L,\ y = 0,\ y = H,\ t > 0$ (12)

This leads to the analytical solution of Eq. (1) for 2D problem as follows:

$$C = C_0 - \frac{16C_0}{\pi^2} \sum_{m=0}^{\infty} \sum_{n=0}^{\infty} A_{mn} \sin\left(\frac{(2n+1)\pi x}{L} \right) \sin\left(\frac{(2m+1)\pi y}{H} \right) F(t) \quad (13)$$

where,

$$F(t) = \exp\left\{ -D\left[\left(\frac{(2n+1)\pi}{L} \right)^2 + \left(\frac{(2m+1)\pi}{H} \right)^2 \right] t \right\} \quad (16)$$

and,

$$A_{mn} = \left(\frac{1}{2n+1} \right) \left(\frac{1}{2m+1} \right) \quad (14)$$

It should be noted that application of this closed-form analytical solution is restricted to simple boundary and initial conditions. Accordingly, developing a numerical approach is necessary for real-life applications.

4. Results and Discussion

The service life is defined as the length of the time elapsing before the chloride content reaches to the maximum limit of chloride on the surface of reinforcements. At this time, the corrosion initiation phase changes to corrosion propagation phase. The corrosion productions are increased on the reinforcements in the corrosion propagation phase, and then the cracks begin to form at the surface of concrete. Initially, to compare the actual error with the closed-form solution, a constant diffusion coefficient is assumed and the solutions of EFGM, FEM, FDM and analytical solution are compared. Subsequently, the service life for a practical problem can be investigated, using the diffusion coefficient as a function of time.

It should be noted that due to the symmetry of the domain, half and a quarter of the models are considered in 1D and 2D problems, respectively. As a result, the Dirichlet boundary condition was applied only to one/two sides of the 1D/2D models, respectively, while the other sides follow the Neumann boundary conditions.

4.1. 1D Problem

In this example, the chloride ingress in a slab shown in Fig. 1 is investigated. The problem specifications are: Thickness =1000 mm, Cover = 50 mm, $D = D_{ref}$ for each design mixtures, and C_t = 0.07 % that is the threshold value of chloride by weight of concrete in the south of Iran [27, 28]. In order to simulate a constant diffusion coefficient, the constant, m, in Eq. (2) is set to zero, and the annual temperature history is assumed to be constant.

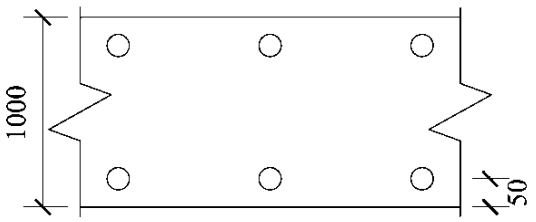

Fig. 1. Cross-section of slab.

In EFG calculations, the scaling parameter of the support domain (d_{max}) and the dilation parameter (K_{ch}) are optimized by using displacement error (L_2) and energy error (H_1) defined as [2]:

$$L_2 = \left[\int_{\Omega} (C_{exact} - C^h)^{\mathrm{T}} (C_{exact} - C^h) \mathrm{d}\Omega\right]^{1/2} \quad (15)$$

$$H_1 = \left[\int_{\Omega} (C_{exact,i} - C_{,i}^{\ h})^{\mathrm{T}} (C_{exact,i} - C_{,i}^{\ h}) \mathrm{d}\Omega\right]^{1/2} \quad (16)$$

where, C and $C_{,i}$ present the chloride content and its derivative, respectively.

To calculate the results at 20 years, half of the slab is divided into 20 equal finite elements (21 nodes) and the same pattern of nodes is considered for FDM and EFG methods. The displacement error (L_2) and energy error (H_1) in EFG method at time = 20 years with various d_{max} and K_{ch} are shown in Figs. 2 and 3, respectively.

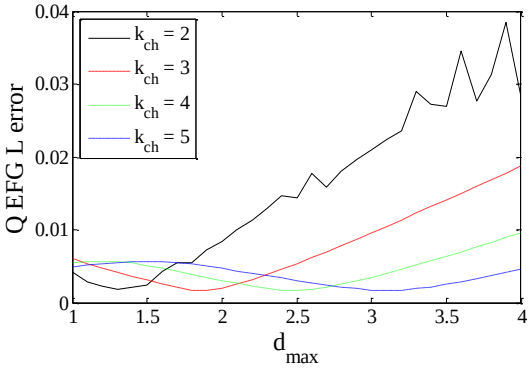

Fig. 2. Q EFG L error estimation using exponential weight function (21 nodes).

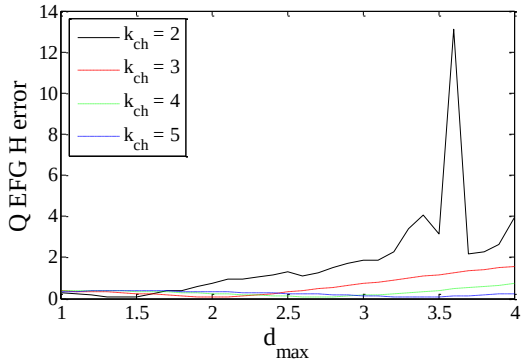

Fig. 3. Q EFG H error estimation using exponential weight function (21 nodes).

It can be concluded that the optimum d_{max} and K_{ch} are equal to 2.5 and 4, respectively. The chloride content-depth and the chloride content-time diagrams are shown in Figs. 4 and 5, respectively.

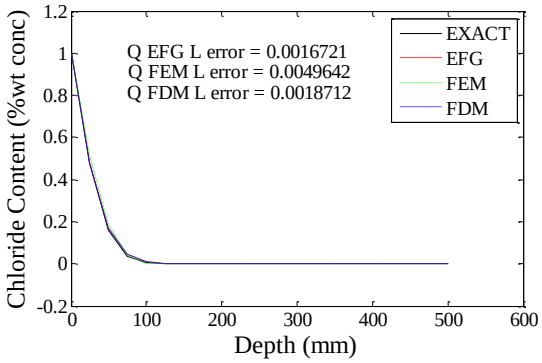

Fig. 4. Chloride content-Depth in cover depth = 50 mm (21 nodes).

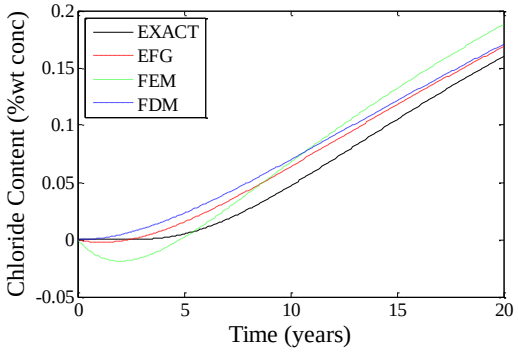

Fig. 5. Chloride content-Time at time = 20 years (21 nodes).

As expected, by increasing the numbers of elements to 100, the numerical methods consistently converge to the analytical solution (EXACT) as indicated in Figs. 6 and 7.

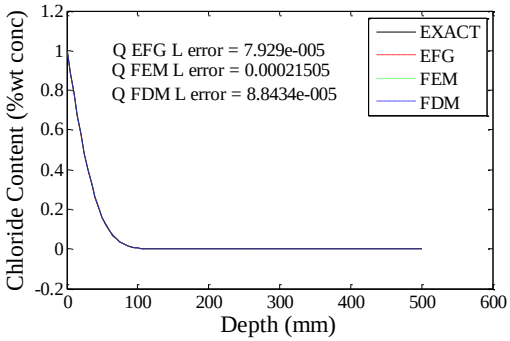

Fig. 6. Chloride content-Depth in cover depth = 50 mm (101 nodes).

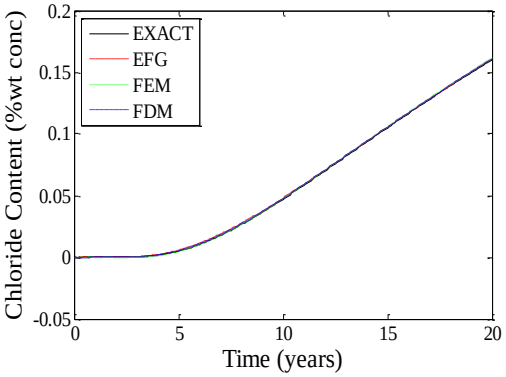

Fig. 7. Chloride content-Time at time = 20 years (101 nodes).

The displacement and energy errors of FDM, FEM and EFG methods are compared with analytical solutions in Table 2.

Table 2. Energy and displacement errors in example 1 at time=20 years.

	Number of nodes	**FDM**	**FEM**	**EFG**
L_2 error (%)	21	0.0018712	0.0049642	0.0016721
	101	8.843e-5	0.0021505	7.929e-5
H_2 error (%)	21	0.195	0.34548	0.10422
	101	0.010211	0.017116	0.0039869

To calculate the results at the corrosion initiation time, half of the slab is divided into 20 and 100 equal elements. The results for 20 elements are shown in Figs. 8 and 9.

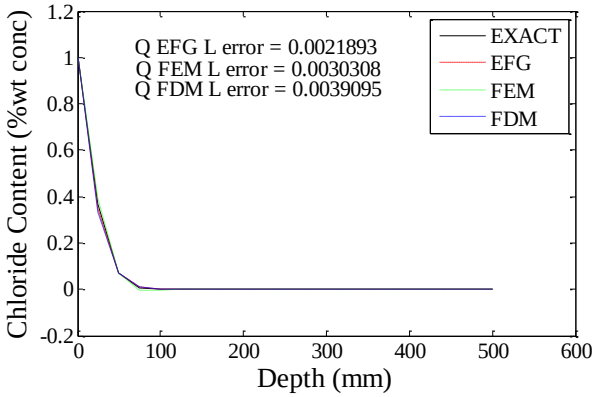

Fig. 8. Chloride content-Depth at corrosion initiation time (21 nodes).

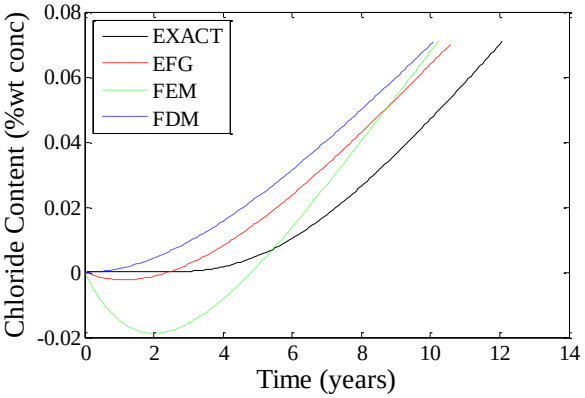

Fig. 9. Chloride content-Time in cover depth = 50 mm (21 nodes).

The corrosion initiation times obtained with different methods are compared in Table 3.

Table 3. Initiation time in example 1.

	Number of Nodes	FDM	FEM	EFG	Exact
Initiation time (year)	21	10.0833	10.25	10.5833	12.0833
	101	12	12	12	12.0833

There is no practical difference between the results obtained by different methods for 100 elements.

A non-consistent diffusion coefficient is also performed by considering the annual average temperature history [18] and setting the constant m to 0.24. As discussed above, no analytical solution is available for this problem. Therefore, in order to estimate the exact solution, the number of elements must be substantially increased. The results are evaluated at the corrosion initiation time of steel bars by dividing the half of the slab into 20 and 100 elements, as depicted in Figs. 10 and 11, for 20 elements.

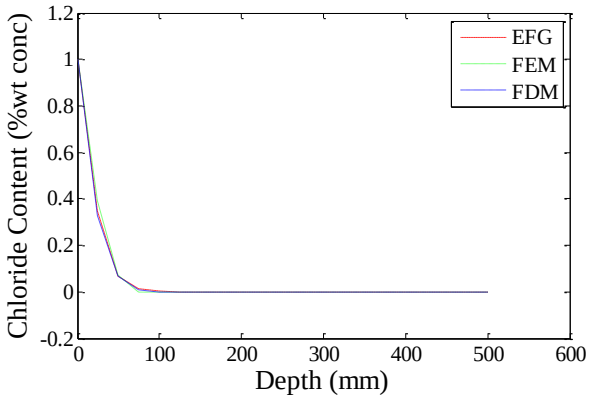

Fig. 10. Chloride content-Depth at corrosion initiation time (21 nodes).

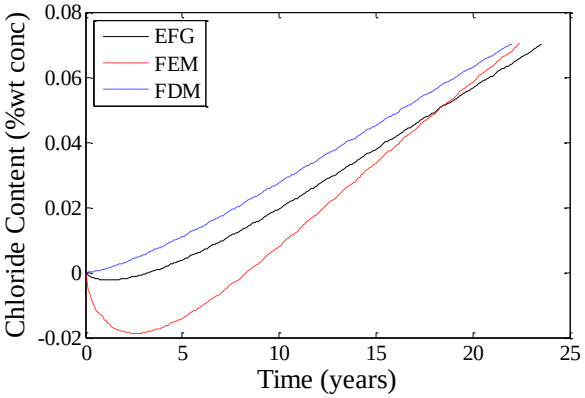

Fig. 11. Chloride content-Time in cover depth = 50 mm (21 nodes).

The corrosion initiation times obtained with different methods are compared in Table 4.

Table 4. Initiation time in example 1.

	Number of Nodes	FDM	FEM	EFG
Initiation time (year)	21	22	22.4167	23.5833
	101	27.6667	27.75	27.6667

The results show that the EFG solution is the most accurate between different models. It should be noted that the EFG procedure is more straightforward in comparison to other methods. The EFG solution is a simple approach to implement as well as being computationally inexpensive.

4.2. 2D Problem

In this section, the chloride ingress in a column depicted in Fig. 12 is investigated. The problem specifications are: Cover = 50 mm, $D = D_{ref}$ for each design mixture, and C_t = 0.07 % (by mass of concrete) that is the threshold value of chloride for south side of Iran [22, 26].

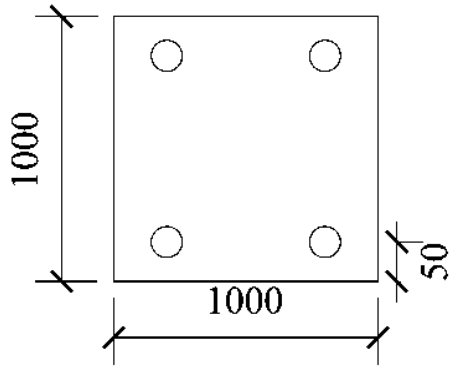

Fig. 12. Cross section of column.

First, the results at 20 years were calculated assuming constant diffusion coefficient (m = 0) and constant 27 ^{o}C annual temperature in a marine site located in Bandar Abbas. In FEM, a quarter of the column section is divided into 328 triangular elements, (with 185 nodes), and the same number of nodes are used in the EFG method. In FDM, a structural 11×11 grid with 121 nodes is used (Fig. 13 a, Fig. 13 b).

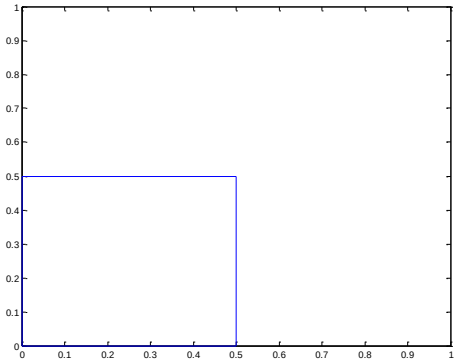

(a)

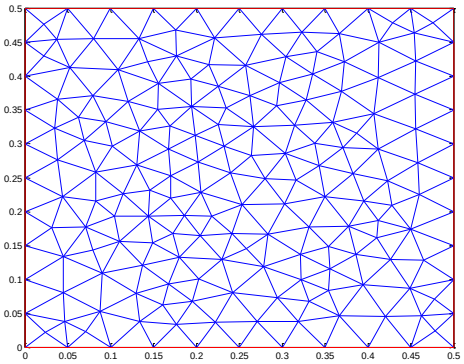

(b)

Fig. 13. a. A quarter of the column section;

b. Triangular elements

The same 1D optimized values of 2.5 and 4 are chosen for d_{max} and k_{ch} , respectively. The calculated chloride profile on the quarter of the column section at 20 years and the chloride profile on the reinforcement at the duration of 20 years are shown in Fig. 14 a to Fig. 14 d.

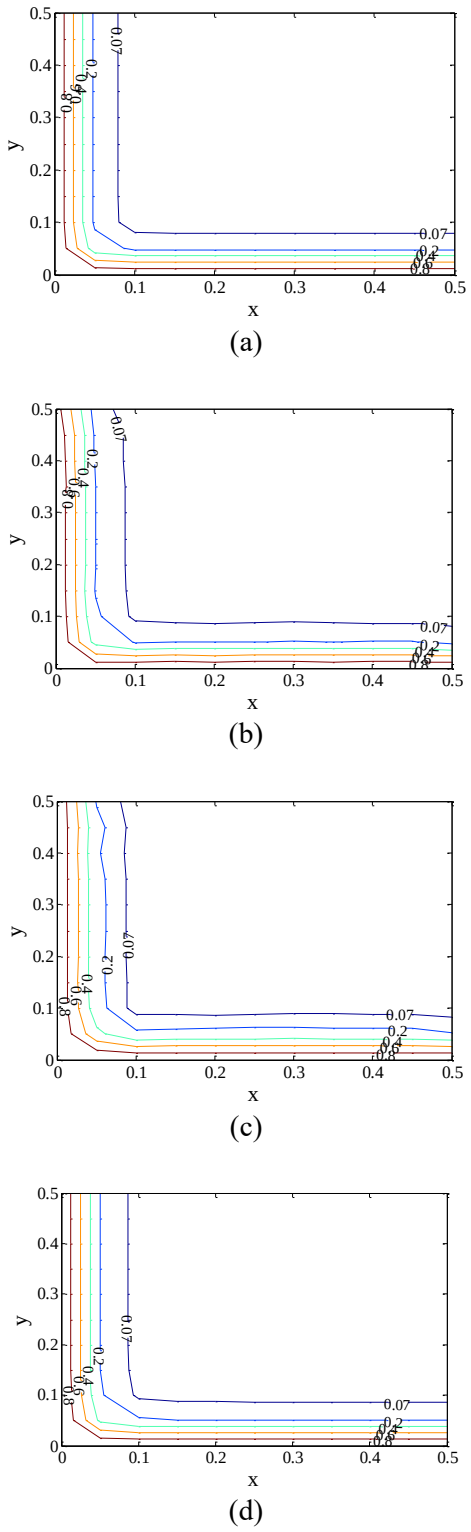

Fig. 14. Chloride content-Depth at time=20 years with analytical method, EFG, FEM, and FDM methods (185 nodes): **a** Analytical method; **b** EFG method; **c** FEM method; d FDM method.

By increasing the number of elements and nodes to 1312 and 697, respectively, and refining the rectangular grid to a 25×25 mesh with 676 nodes in FDM, all numerical solutions converge to the analytical solution as shown in Fig. 15 a and Fig. 15 b.

The displacement errors of the FDM, FEM and EFG methods are compared in Table 5.

Table 5. Displacement error in Example 2 at time=20 year.

	Number of Nodes	**FDM**	**FEM**	**EFG**
L_2 error (%)	185	0.0074	0.0144	0.0074
	697	9.8107e-4	0.0048	0.0027

Because of using rectangular type of mesh in FDM, the displacement error in FDM is less than the EFG method and FEM that used triangular mesh. This results in some calculation errors in determining the L_2 error is due to use of rectangular Gaussian points. When using rectangular mesh, the L_2 error for EFG method becomes 0.00083 instead of 0.0027. Although the L_2 error is lower in the case of a rectangular mesh, this does not necessarily indicate that the rectangular mesh is more accurate than the triangular mesh. It should be noted that when transferring the results from triangular nodes to rectangular nodes in the calculation of the L_2 error, some errors can be introduced into the solution.

The results of the corrosion initiation time of steel bars are also shown in Fig. 15 c and Fig. 15 d.

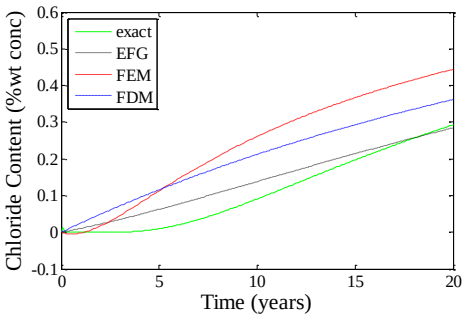

(a)

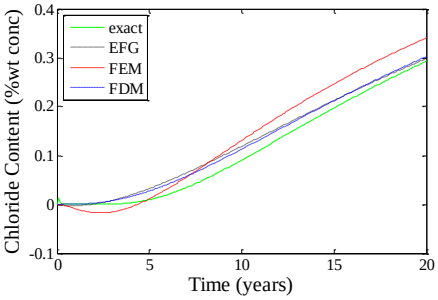

(b)

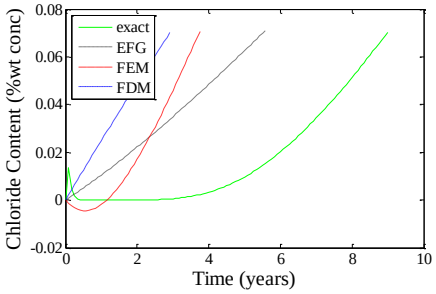

(c)

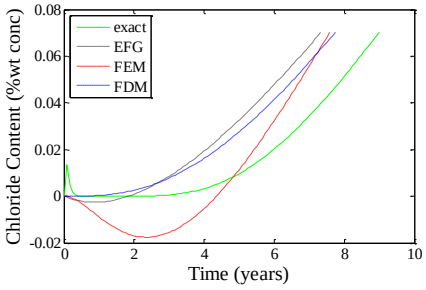

(d)

Fig. 15. Chloride content-Time in cover depth = 50 mm, Rectangular Mesh: **a** 185 nodes; **b** 697 nodes; Triangular Mesh: **c** 185 nodes; **d** 697 nodes.

The corrosion initiation time obtained using different methods are compared in Table 6.

Table 6. Corrosion initiation time in Example 2.

	Number of Nodes	FDM	FEM	EFG	Exact
Corrosion initiation time (year)	185	2.9167	3.75	5.5833	9
	697	7.75	7.5833	7.3333	9

Finally, a non-consistent diffusion coefficient problem using the annual average temperature history of Bandar Abbas, Iran [19] and m = 0.24 is re-considered. As it is described in 1D, there is no available analytical solution, while the exact solution can be estimated by increasing the number of elements.

Using geometric modeling similar to the last case, the results of the corrosion initiation time of steel bars are evaluated in Fig. 16 a and Fig. 16 b.

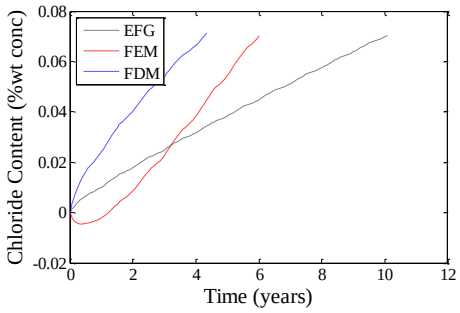

(a)

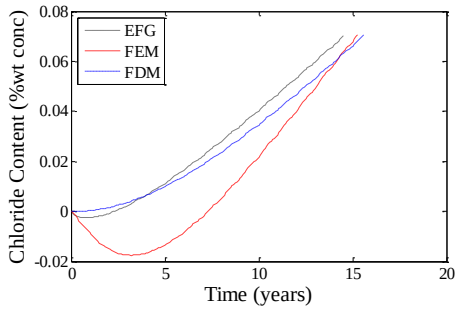

(b)

Fig. 16. Chloride content-Time in cover depth = 50 mm: **a** 185 nodes; **b** 697 nodes.

The corrosion initiation times of the steel bars, calculated by different methods, are compared in Table 7.

Table 7. Initiation time in Example 2.

	Number of Nodes	FDM	FEM	EFG
Corrosion initiation time (year)	185	4.3333	6	10.0833
	697	15.5833	15.25	14.5

Fig. 17 and Table 7 indicate that the EFG method error is lower than the other methods when 185 nodes are used for solving the problem. Comparing the discussed different methods indicates that the corrosion initiation time predicted by EFG method is much closer to the actual corrosion initiation time. All methods converge to the exact solution by increasing the number of nodes.

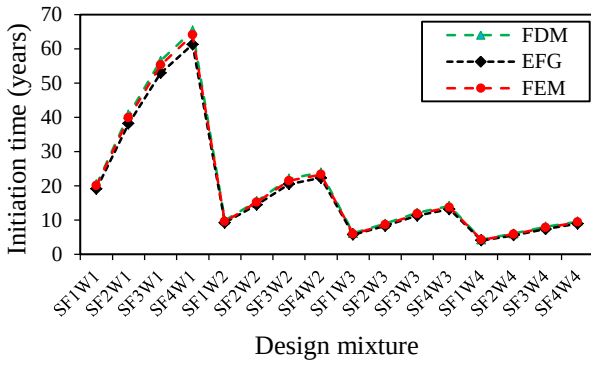

Fig. 17. Initiation time-Design mixture in cover depth = 50 mm (697 nodes).

Furthermore, comparing the necessary computing time to solve the 2D equation (Table 8) using different approaches shows that FDM is the fast computational approach among the other mentioned methods.

The results above discussed were obtained from a mixture design with a 0.40 water-to-binder ratio and a concrete using 7.5% silica fume content as a replacement of Portland cement.

Table 8. Computing time for a 2D non-constant *D* problem in Example 2.

	Number of Nodes	FDM	FEM	EFG
Computing time (s)	185	0.1700	1.9300	1.8890
	697	0.3440	32.9040	14.9140

Below, the EFG, FEM and FDM outcomes are compared with each other for all mixture designs with the water-to-binder ratios, including 0.35 (W1), 0.40 (W2), 0.45 (W3) and 0.50 (W4), and substitution of the silica fume content in concrete, including 5 % (SF1), 7.5 % (SF2), 10 % (SF3) and 12.5 % (SF4). Fig. 17 shows the corrosion initiation time of silica fume concrete for a covering depth of 50 mm. This estimate is based on the proposed diffusion model. The threshold chloride value in the south of Iran is supposed to be 0.07 % by weight of concrete [29]. The results indicate that the use of silica fume as a replacement of Portland cement in concrete can increase the corrosion initial time. Additionally, due to the low permeability of concrete in a lower w/b ratio, superior corrosion resistance can be obtained. Thus, the most effective way to decrease the chloride diffusion in concrete is reducing the w/b ratio and increasing the silica fume replacement in concrete.

5. Conclusion

In this paper, FDM, FEM and EFG methods were adopted to solve Fick's Second Law by using the diffusion model as a function of temperature, time, water-to-binder ratio and

silica fume content, and the reference diffusion coefficient. In the first step, the scaling parameter of support domain (d_{max}) and the weight function's dilation parameter (K_{ch}) were optimized by minimizing the displacement error (L_2) and energy error (H_1). Then, by applying these parameters to the EFG method, the results were compared with those obtained by FDM, FEM, and available analytical solution. It was shown that the EFG method predicts the service life more accurately than the other methods, and exhibits the lowest displacement error and energy error for a constant diffusion coefficient problem. FDM can be performed very efficiently for simple models, and the displacement error produced by this method does not differ considerably from the EFG results. Therefore, FDM could compete with the EFG method in simple geometries. FEM can be used with a sufficient number of elements while the convergence of the results should be controlled. However, in complicated models, FEM and especially the EFG method are much more flexible than FDM.

For practical problems where the diffusion coefficient is inconsistent, having an insufficient number of elements leads to a considerable number of errors, especially in 2D conditions. The EFG method is found to be less sensitive as compared to other investigated numerical methods.

These methods for solving the partial differential equations of chloride diffusion are the parabolic initial boundary value problems, and may be applied for other similar physical phenomena, such as soil consolidation, heat transfer, etc.

REFERENCES

[1] Rodriguez, O.G., Hooton, R.D. (2003). "Influence of Cracks on Chloride Ingress into Concrete." ACI Mater. J., Vol. 100, pp. 120-126.

[2] Bitaraf, M., Mohammadi, S. (2008). "Analysis of chloride diffusion in concrete structures for prediction of initiation time of corrosion using a new meshless approach." Constr. Build. Mater., Vol. 22, pp. 546-556.

[3] Goltermann, P. (2003). "Chloride ingress in concrete structures; extrapolation of observations." ACI Mater. J., Vol. 100, pp. 114-119.

[4] Oh, B.H., Jang, B.S. (2003). "Chloride diffusion analysis of concrete structures considering effects of reinforcements." ACI Mater. J., Vol. 100, pp. 143-149.

[5] Garber, D., Shahrokhinasab, E. (2019). Performance Comparison of In-Service, Full-Depth Precast Concrete Deck Panels to Cast-in-Place Decks (No. ABC-UTC-2013-C3-FIU03-Final). Accelerated Bridge Construction University Transportation Center (ABC-UTC).

[6] Ehlen, M.A. (2012). "Life-365TM Service life prediction model and computer program for predicting the service life and life-cycle cost of reinforced concrete exposed to chlorides, Manual of Life-365TM." Version 2.1, Life-365™ Consortium II.

[7] Zienkiewicz, O.C., Taylor, R.L., Zhu, J.Z. (2005). "The finite element method: its basis and fundamentals." Elsevier Butterworth-Heinemann, Amsterdam, United Kingdom.

[8] Li, C., Ding, H. (2014). "Higher order finite difference method for the reaction and anomalous-diffusion equation." Appl. Math Modelling. Vol. 38(15-16), pp. 3802-3821.

[9] Trobec, R., Kosec, G., Sterk, M., Sarler, B. (2012). "Comparison of local weak and strong form meshless methods for 2D diffusion equation." Eng. Anal. Bound. Elem., Vol. 36, pp. 310-321.

[10] Nayroles, B., Touzot, G., Villon, P. (1992). "Generalizing the finite element method: diffuse approximation and diffuse elements." Comput. Mech., Vol. 10, pp. 307-318.

[11] Dehghan, M., Abbaszadeh, M., Mohebbi, A. (2016). "Analysis of two methods based on

Galerkin weak form for fractional diffusion-wave: Meshless interpolating element free Galerkin (IEFG) and finite element methods." Eng. Anal. Bound. Elem., Vol. 64, pp. 205-221.

[12] Liu, W.K., Adee, J., Jun, S. (1993). "Reproducing kernel and wavelet particle methods for elastic and plastic problems." ASME. Vol. 33, pp. 175-190.

[13] Iqbal, M., Gimperlein, H., Mohamed, M.S., Laghrouche, O. (2015). "An investigation of the accuracy of the partition of unity method for time dependent heat transfer problems." Infrastructure and Environment Scotland 3rd Postgraduate Conference, Heriot-Watt University, Edinburgh.

[14] Lehoucq, R.B., Narcowich, F.J., Rowe, S.T., Ward, J.D. (2018). "A Meshless Galerkin Method For Non-Local Diffusion Using Localized Kernel Bases." Math. Comp., Vol. 87, pp. 2233-2258.

[15] Zhang, T., Li, X. (2017). "A variational multiscale interpolating element-free Galerkin method for convection-diffusion and Stokes problems." Eng. Anal. Bound. Elem., Vol. 82, pp. 185-193.

[16] Ingber, M.S., Chen, C.S., Tanski, J.A. (2004). "A mesh free approach using radial basis functions and parallel domain decomposition for solving three-dimensional diffusion equations." Int. J. Numer. Methods Engrg., Vol. 60, pp. 2183-2201.

[17] Gyrya, V., Lipnikov, K., Manzini, G. (2016). "The arbitrary order mixed mimetic finite difference method for the diffusion equation." ESAIM: M2AN., Vol. 50(3), pp. 851-877.

[18] Yang, Y., Huang, Z. (2016). "Tailored Finite Point Method for Parabolic Problems." Comput. Methods Appl. Math., Vol. 16(4), pp. 543-562.

[19] Farahani, A., Taghaddos, H., Shekarchi, M. (2015). "Prediction of long-term chloride diffusion in silica fume concrete in a marine environment." Cem. Concr. Compos., Vol. 59, pp. 10-17.

[20] Azizi Moghaddam, B. (2005). "Study on the time-dependent diffusion of chloride ion into concrete in different exposure conditions using various concrete coating." M.Sc. Thesis, University of Tehran, Tehran.

[21] Chini, M., Ghods, P., Alizadeh, R., Hoseini, M., Montazer, Sh., Shekarchi, M., Ghalibafian, M. (2004). "Developing the first version of the model for service life prediction of reinforced concrete structures in Persian Gulf and Oman Sea." 2nd report, NO. CMI 8309144: Construction Materials Institute at the University of Tehran, Iran.

[22] Shekarchi, M., Alizadeh, R., Ghods, P., Chini, M., Hosseini, M. (2008a). "Durability based design of RC structures in south of Iran using DuraPGulf model." Arab J. Sci. Eng., Vol. 33, pp. 77-88.

[23] Shekarchi, M., Ghods, P., Alizadeh, R., Chini, M., Hoseini, M. (2008b). "DuraPGulf, a local service life model for the durability of concrete structures in the south of Iran." Arab J. Sci. Eng., Vol. 33, pp. 77-88.

[24] Crank, J. (1995). "The Mathematics of Diffusion." Second ed. Oxford: Oxford Science Publications, London.

[25] Gresho, P.M., Sani, R.L. (2000). "Incompressible flaw and the Finite Element Method." Vol. 1, Advection-Diffusion and Isothermal Laminar Flaw, John Wiley & Sons.

[26] Cheng-Kong, C.W., Michael, E.P. (2002). "Essential boundary condition enforcement in mesh less methods: boundary flux collocation method." Int. J. Numer. Methods Engrg., Vol. 53, pp. 499-514.

[27] Farahani, A., Taghaddos, H., Shekarchi, M. (2018). "Chloride diffusion modeling in pozzolanic concrete in marine site." ACI Mater. J., Vol. 115(4), pp. 509-518.

[28] Shekarchi, M., Moradi-Marani, M., Pargar, F. (2011). "Corrosion damage of reinforced concrete jetty structure in the Persian Gulf: A case study." Struct. Infrastruct. Eng., Vol. 7, pp. 701-713.

[29] Ghods, P., Alizadeh, R., Chini, M., Hoseini, M., Ghalibafian, M., Shekarchi, M. (2007). "Durability-based design in the Persian Gulf." Concr. Int., pp. 50-55.